Free Radical Research, June 2006; 40(6): 647–658

The fate of olive oil polyphenols in the gastrointestinal tract: Implications of gastric and colonic microflora-dependent biotransformation

GIULIA CORONA[1,2], XENOFON TZOUNIS[1], M. ASSUNTA DESSÌ[2], MONICA DEIANA[2], EDWARD S. DEBNAM[3], FRANCESCO VISIOLI[4] & JEREMY P. E. SPENCER[1]

[1]*Molecular Nutrition Group, School of Food Biosciences, University of Reading, Reading RG6 6AP, UK,* [2]*Dipartimento di Biologia Sperimentale, Sez. Patologia Sperimentale, Università degli Studi di Cagliari, Monserrato 09042, Italy,* [3]*Department of Physiology, Royal Free and University College Medical School, London, UK, and* [4]*Department of Pharmacological Sciences, University of Milan, Milan 20133, Italy*

Accepted by Professor B. Halliwell

(Received 5 August 2005; in revised form 5 September 2005)

Abstract

We have conducted a detailed investigation into the absorption, metabolism and microflora-dependent transformation of hydroxytyrosol (HT), tyrosol (TYR) and their conjugated forms, such as oleuropein (OL). Conjugated forms underwent rapid hydrolysis under gastric conditions, resulting in significant increases in the amount of free HT and TYR entering the small intestine. Both HT and TYR transferred across human Caco-2 cell monolayers and rat segments of jejunum and ileum and were subject to classic phase I/II biotransformation. The major metabolites identified were an *O*-methylated derivative of HT, glucuronides of HT and TYR and a novel glutathionylated conjugate of HT. In contrast, there was no absorption of OL in either model. However, OL was rapidly degraded by the colonic microflora resulting in the formation of HT. Our study provides additional information regarding the breakdown of complex olive oil polyphenols in the GI tract, in particular the stomach and the large intestine.

Keywords: *Olive oil, hydroxytyrosol, tyrosol, absorption, metabolism, colonic microflora*

Introduction

Olive oil is the principal fat component of the mediterranean diet and its consumption has been associated with a lower incidence of coronary heart disease and certain cancers [1–4]. Extra virgin olive oil contains a variety of simple phenolic compounds, such as hydroxytyrosol (HT), tyrosol (TYR), and their secoiridoid derivatives, such as oleuropein (OL) (Figure 1). Secoiridoids are a group of coumarin-like compounds, which are usually glycosidically bound that are produced from the secondary metabolism of terpenes as precursors of various indole alkaloids. The secoiridoids in olive oil are mainly derived from the oleoside type of glucoside, which are characterized by an exocyclic 8,9-olefinic functionality, a combination of elenolic acid and a glucosidic residue (Figure 1). OL is an ester of HT and the oleosidic skeleton. These compounds, together with other components, such as tocopherols, contribute towards the protection of olive oil against auto-oxidation, and have been demonstrated to exert many potentially beneficial biological effects both *in vitro* and *in vivo* [5–11].

However, the biological properties of these compounds *in vivo* will depend on the extent of their absorption and metabolism. *In vivo* studies have been performed to investigate the bioavailability of olive oil

Correspondence: J. P. E. Spencer, School of Food Biosciences, University of Reading, PO Box 226, Whiteknights, Reading RG6 6AP, UK. Tel: 44 118 378 8724. Fax: 44 118 931 0080. E-mail: j.p.e.spencer@reading.ac.uk

ISSN 1071-5762 print/ISSN 1029-2470 online © 2006 Taylor & Francis
DOI: 10.1080/10715760500373000

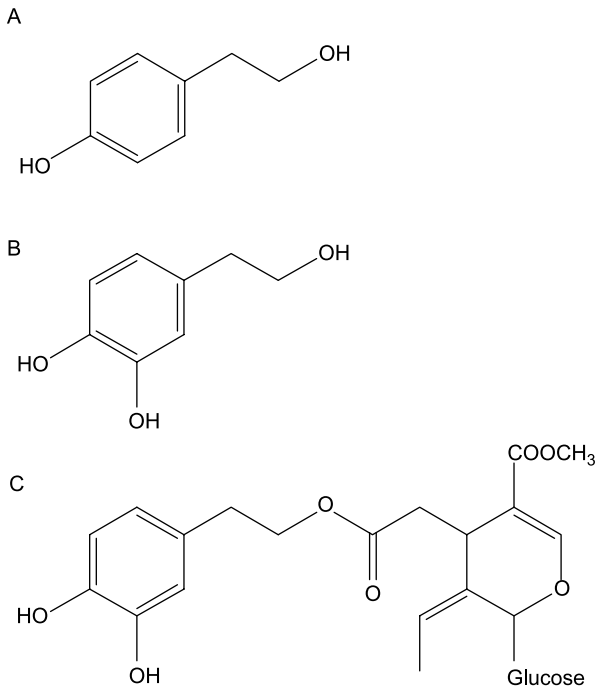

Figure 1. Structures of olive oil polyphenols. (A) TYR; (B) HT and (C) OL.

polyphenols by measurement of their excretion in urine following administration [12–15]. It has been reported that HT and TYR levels in urine increase after olive oil administration, and that these compounds were primarily excreted as *O*-glucuronidated conjugates [15–17]. HT may also be *O*-methylated *in vivo*, and homovanillic acid and homovanillyl alcohol have been measured in human and animal studies in plasma and urine after olive oil ingestion [12,16,18,19]. In addition, human studies conducted in healthy and ileostomy patients fed with polyphenols have provided evidence that ingested olive oil phenols were absorbed in healthy and ileostomy subjects, indicating that most, if not all, are absorbed in the small intestine [20]. However, only few data exist for the absorption and metabolism of olive oil polyphenols in the small intestine, and there are little or no data for their stability in the stomach or their biotransformation in the colon. For example, Manna et al. [21] reported that HT is absorbed by passive diffusion in Caco-2 cells but there are no data on the specific absorption/metabolism of other olive oil polyphenols in the small intestine.

The aim of this study was to investigate the absorption, subsequent biotransformation and potential modification of a range of olive oil polyphenols (including OL and secoiridoid derivatives) in the gastrointestinal tract. In particular we focus on their decomposition in the stomach, their absorption and metabolism in the small intestine and their biotransformation by the microflora present in the large intestine. Knowledge of the detailed biotransformation of olive oil polyphenols in the gastrointestinal tract will provide important information regarding potential bioactive components *in vivo*.

Materials and methods

Materials

The polyphenolic mixture was obtained by processing extra virgin olive oil by methanol/water extraction as previously described by Caruso et al. [17]. The Caco-2 cell line was obtained from ECACC (Salisbury, Wiltshire UK). TYR and OL were obtained from Extrasynthase (ZI Lyon Nord, Genay, France). HT was obtained from Cayman Chemical Company (Ann Arbor, MI). β-Glucuronidase (type L-II from limpets) was purchased from Sigma (Poole, Dorset, UK). Peptone water, yeast extract and bile salts were purchased from Oxoid Ltd. (Basingstoke, UK). HPLC grade acetonitrile and methanol were purchased from Fisher (Hampton, NH) and Elgstat UHP double distilled water (18.2 Ω grade) was used throughout the study. HPLC columns were purchased from Waters (Watford, Herts, UK). All other reagents used were obtained from Sigma.

Incubation of polyphenolic fraction with simulated gastric juice

In order to obtain information about the breakdown susceptibility of conjugated forms, polyphenolic fraction (1 mg/ml) was submitted to acidic hydrolysis under conditions similar to the gastric environment (water acidified with HCl to reach pH 2) and incubated at 37°C for 30 min, 1, 2 and 4 h. After incubation, samples were analyzed by HPLC detection (see later). As water at pH 2 has no buffering capacity, it is possible that the pH will rise as hydrolysis occurs. We monitored the pH during experiments and it was found not to increase significantly during the experimental incubation time (up to 4 h).

Transport and metabolism experiments in the perfused rat intestinal model

Transport and metabolism experiments were conducted using the *in vitro* intestinal preparation of Fisher and Gardner [22,23] in which the lumen of isolated intestine is perfused with a segmental flow (defined as perfusion of buffer interspersed with bubbles of the gas mixture) of bicarbonate buffer (pH 7.4) equilibrated with 95% O_2:5% CO_2 and containing 28 mM glucose. The bicarbonate buffer consisted of HCO_3^- 25 mM; Na^+143 mM; Cl^- 133.7 mM; K^+5.9 mM; HPO^{4-} 1.2 mM; Ca^{2+}2 mM and Mg^{2+}1.2 mM. Male Sprague–Dawley rats (230–260 g) were anaesthetized with pentobarbital

sodium (90 mg/kg, intra-peritoneally) and sections of jejunum (20–30 cm long, beginning 10 cm from the ligament of Treitz) or ileum (20–30 cm long, ending 5 cm from the ileo-caecal junction) were cannulated and the lumen was segmentally perfused with the buffer described above. The intestinal sections were then removed from the animal by stripping them from the mesentery, and suspended in a chamber containing liquid paraffin at 37°C whilst maintaining the segmental flow of buffer. Before transport experiments were started, the segments were perfused for 40 min in order to flush blood from the vasculature and to allow fluid absorption to reach a steady state. Thereafter, HT (54 μM), TYR (62.5 μM), OL (100 μM) and polyphenolic fraction (18 mg/l) were added to the buffer and perfused through the intestinal segment, in a single pass fashion, for up to 80 min. During perfusion, absorbed fluid dropped through the paraffin to the base of the chamber and was collected at timed intervals of 20 min. Samples collected from both the jejunum and the ileum were immediately stored at −20°C until analysis. The presence of glucuronide conjugates in the gut samples was established by treatment with ß-glucuronidase. Incubation of samples with enzyme (2000 units/ml) was for 120 min at 37°C in a 0.1 M sodium phosphate buffer, pH 3.8. The 0.1 M phosphate buffer effectively inhibits all sulphatase activity that the enzyme possesses. A glucuronide of an unknown TYR metabolite has been characterized and quantified at 280 nm with TYR as the reference compound.

Cell culture

Sub-cultures of the Caco-2 cells were grown in T-75 culture flasks and passaged with a trypsin-versene solution. Cells were cultured in DMEM supplemented with 20% FBS, 1% non essential amino acids, 2 mM L-glutamine, penicillin (100 units/ml) and streptomycin (100 g/ml) at 37°C in 5% CO_2.

Transport experiments in the human Caco-2 cell culture model

For all transcellular transport studies, Caco-2 cells were seeded in 12 mm i.d. Transwell inserts (polycarbonate membrane, 0.4 μm pore size; Corning Costar Corp.) in 12-well plates at a density of 5×10^4 cells/ml. The basolateral (serosal) and apical (mucosal) compartments contained 1.5 and 0.5 ml of culture medium, respectively. Culture medium was replaced three times a week for 21 days. Before the transport experiment media in both chambers was replaced with Hepes-buffered medium (HBM; pH 7.4; 5 mM Hepes, 154 mM NaCl, 4.6 mM KCl, 33 mM glucose, 5 mM $NaHCO_3$, 1.2 mM Na_2HPO_4). Caco-2 cells in transwells at passage 25–40 were used for transport experiments at 21 days post seeding. Only inserts with transepithelial electrical resistance (TEER) values $>300\,\Omega/cm^2$ were used for transport experiments. Different concentrations of HT, TYR and OL (10, 50 and 100 μM) and POL (5, 25 and 50 μg/ml) in methanol were added in the apical side and upon termination of the 2 h incubation at 37°C, samples from both compartments were collected for immediate HPLC analysis. Control experiments to monitor the oxidation of HT, TYR, OL and the olive oil fraction in medium alone (i.e. in the absence of cells) were performed and indicated no significant loss of any of the polyphenols for up to 4 h post addition.

Synthesis of hydroxytyrosol–glutathione conjugate

Hydroxytyrosol–glutathione conjugate was prepared by a method similar to that previously described by Spencer et al. [24] for catecholamine conjugates, with some modifications. GSH (10 mM) and mushroom tyrosinase (2000 units/ml) were incubated in sodium acetate buffer (20 mM), pH 6.5, at 25°C (total volume of 10 ml) before the drop-wise addition of HT (10 mM) under constant stirring for 1 h. To stop the reaction, the sample mixture was acidified with 0.5% HCl 5 M and after centrifugation the supernatant was collected for HPLC analysis.

Colonic microflora fermentation: Batch culture

The composition of the basal growth medium, per liter, was: peptone (2 g), yeast extract (2 g), Tween 80 (2 ml), hemin (50 mg), vitamin K1 (10 μl), L-cysteine HCl (0.5 g), bile salts (0.5 g), NaCl (0.1 g), $NaHCO_3$ (2 g), K_2HPO_4 (40 mg), KH_2PO_4 (40 mg), $MgSO_4^- 7H_2O$ (10 mg), $CaCl_2^- 6H_2O$ (10 mg), resazurin (1 mg) and distilled water to volume. The medium was dispensed into the fermentation vessels and autoclaved at 121°C for 15 min. Post-autoclaving, the hot medium was purged with oxygen-free nitrogen at the rate 15 ml/min. Fecal slurry of 10% (w/v) feces was prepared by homogenizing a stool sample with anaerobic phosphate-buffered saline (0.1 M, pH 7.0) in a stomacher. The slurry was sieved to remove particulate material. Fecal donors were aged 20–40 years, had no history of gastrointestinal disease, and had not taken antibiotics in the 6 months prior to donation. Samples were processed within 10 min of defecation. The fermentation volume was 150 ml. Each batch culture (substrate fermentation and control fermentations) consisted of 90% basal growth medium and 10% fecal slurry. OL (1 mM) was added to the vessel and culture pH was maintained at 6.8–7.0 throughout the incubation. Continuous monitoring of pH and automatic addition of alkali (0.5 M NaOH) and acid (0.5 M HCl) was achieved by use of an Electrolab pH controller. Cultures were incubated at 37°C by a heated water

jacket, continuously purged with oxygen-free nitrogen (15 ml/min) and mixed on a magnetic stirrer. The fermenters were made of glass and had sampling ports to remove culture medium for analysis through the incubations, at time 0, 4, 8, 12, 24 and 48 h. Following sampling from fermentation vessels, the suspension was spun for 5 min at 13,000 × g. The resultant supernatant was used for HPLC analysis. The experiment was carried out in duplicate and using three different fecal donors. Control experiments indicated that there was no oxidation or loss to any of the compounds when incubated in the batch culture medium only.

HPLC analysis

HPLC analysis to measure compound and metabolite concentrations was carried out with a Hewlett-Packard 1100 series liquid chromatograph (Hewlett-Packard, Palo Alto, CA) equipped with a diode array detector linked to the HP ChemStation Software system. Samples were analyzed by reverse-phase HPLC using a Nova-Pak C18 column (4.6 × 250 mm) (Waters Company) with 4 μm particle size. The temperature of the column was maintained at 30°C. The mobile phases consisted of a mixture of aqueous methanol 5% in 0.1% hydrochloric acid 5 M (A) and a mixture of aqueous acetonitrile 50 in 0.1% hydrochloric acid 5 M (B) and were pumped through the column at 0.7 ml/min. The following gradient system was used (min/% B): 0/5, 5/5, 40/50, 55/100, 59,9/100, 60/5, with 10 min post-run for both compound and metabolite detections. The eluent was monitored by photodiode array detection at 280 nm and spectra of products obtained over the 200–600 nm range. Calibration curves of the compounds were constructed using authentic standards (0.1–100 μM) and in each case were found to be linear with correlation coefficients of >0.995.

Calculations and statistics

Apparent permeability coefficients (P_{app}) were calculated with the following equation: $P_{app} = V \times dC/A \times C0 \times dT = [cm/s]$; where $V =$ the volume of the solution in the receiving compartment (ml), $A =$ the membrane surface area (cell system) or intestinal segment surface area (perfused rat intestinal model), $C0 =$ the initial concentration of compound and $dC/dt =$ the change in drug concentration in the receiver solution over time. Intestinal segment surface area was calculated using the equation for the area of a cylinder ($A = 2\pi r_i \times L_i$), where L_i is the length of the perfused segment of intestine and r_i is the internal radius, 0.2 cm [25]. Transport data are expressed as a mean of 3 or more determinations ± SEM.

Results

Incubation of polyphenolic fraction with simulated gastric juice

Although the gastric conditions *in vivo* are complex with the food matrix affecting the precise pH, the incubation of polyphenols at gastric pH can give us information about the stability of polyphenols in the gastric environment. An olive oil polyphenolic fraction (1 mg/ml) was incubated in water acidified with HCl to reach a pH 2 at 37°C for up to 4 h to simulate conditions in the stomach, and the products were analyzed by HPLC with photodiode array detection. The results indicate a time dependent hydrolysis of conjugated polyphenols as demonstrated by a decline of compounds represented by peaks with a retention time (RT) between 40 and 60 min, and a corresponding progressive increase in peaks representing the hydrolysis products HT (RT 12.1 min) and TYR (18.3 min RT), respectively (Figure 2A and B). After 30 min incubation, the amount of HT and TYR increased 4.75 and 3.25 times, respectively, and after 4 h the amount increased 7.41 and 5.15 times, respectively (Figure 2C). Interestingly, after 4 h of hydrolysis, some fractions of the conjugated forms are still present unhydrolyzed. This result indicates that the amount of HT and TYR that arrive in the small intestine following incubation and passage through the acidic conditions of the stomach may be considerably higher than the amount initially present in ingested olive oil.

Transport and metabolism experiments in the perfused rat intestinal model

The comparative absorption of HT, TYR, OL and polyphenolic fraction, and the extents to which they are conjugated and metabolized during transfer across jejunum and ileum to the serosal side was investigated. The transferred compounds were identified and quantified by HPLC with diode array detection. Figure 3 shows the time course for transfer and metabolism of HT (Figure 3A and B), TYR (Figure 3C and D) and the polyphenolic extract (POL) (Figure 3E and F) in jejunum and ileum, respectively. Interestingly, OL was not transferred across either small intestinal segments, at any time point. In contrast, HT (Figure 3A and B) and TYR (Figure 3C and D) were rapidly absorbed in both jejunum and ileum, following perfusion with the single phenolics, and significant amounts of phase I and II metabolites were found in the serosal fluid. After HT perfusion, HT, 3-*O*-methyl-HT (homovanillyl alcohol) and the respective glucuronides of both compounds were detected following jejunum and ileum passage (Figure 3A and B). Similarly, after perfusion with TYR, the parental compound and two new peaks were observed in the serosal fluid of both

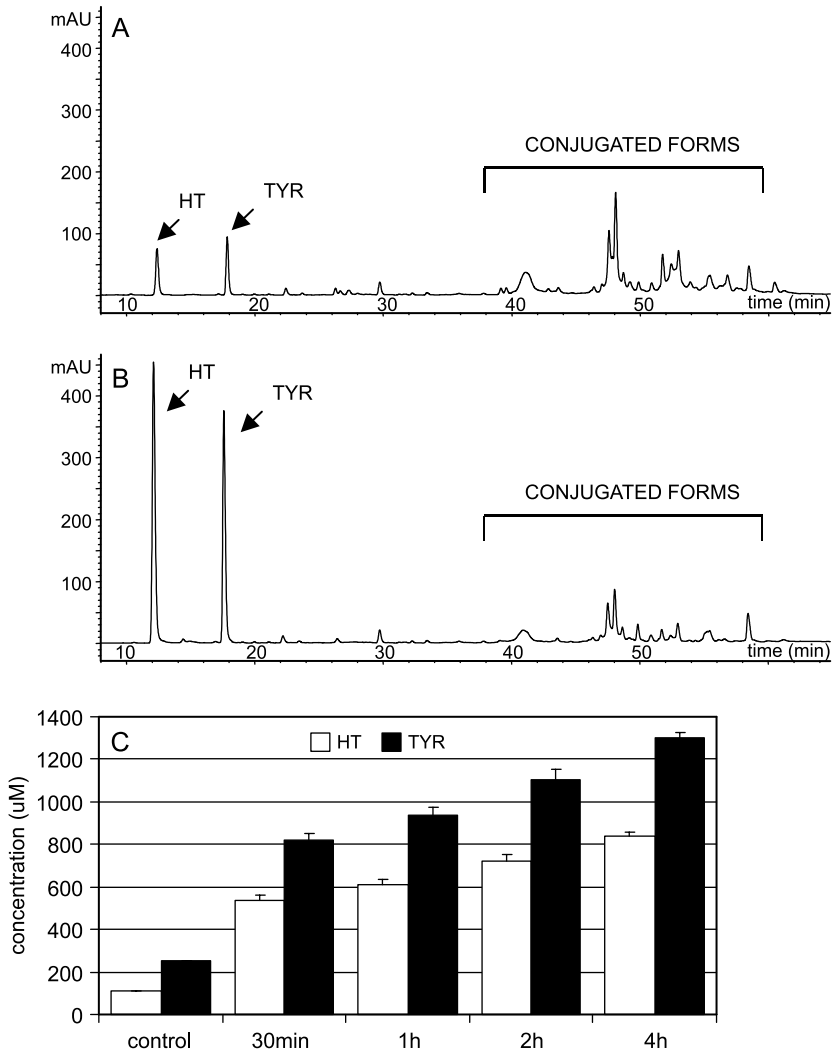

Figure 2. HPLC chromatogram obtained from a control (panel A) and a sample (panel B) after 2 h incubation in HCl. Detection was performed at 280 nm. Amounts of HT and TYR obtained after hydrolytic treatment of olive oil polyphenolic fraction over time (panel C). Data are plotted as the mean ± SEM ($n = 3$) and all values are significantly different respect to the control ($p < 0.001$).

gut segments (Figure 3C and D). Both new peaks disappeared after glucuronidase treatment, with a subsequent increase in TYR and a new peak, indicating that a glucuronide of TYR and another glucuronide metabolite were present. This new peak had similar spectral properties as TYR, but it remains to be identified. Figure 4 indicates that both HT and TYR are absorbed in the parental form to a greater extent in the ileum than in the jejunum (Figure 4A and B), which may reflect enzymatic profiles in these tissues. The perfusion of the polyphenolic fraction also resulted in the transfer of compounds, TYR and HT, and lead to the formation of glucuronide conjugates and homovanillyl alcohol (Figures 3E and F and 4C). HPLC chromatograms did not reveal the presence of other metabolite resulting from the polyphenolic extract perfusion. We calculated the apparent permeability coefficients for HT and TYR in both jejunum (P_{app}[HT] = 1.26 ± 0.52 × 10^{-5}; P_{app}[TYR] = 3.55 ± 0.11 × 10^{-5}) and ileum (P_{app}[HT] = 1.41 ± 0.99 × 10^{-5}; P_{app}[TYR] = 2.91 ± 0.56 × 10^{-5}) (Figure 5), indicating that they are well absorbed in both segments of small intestine.

Transport experiments in Caco-2 model

Analysis by HPLC of apical (AP) and basolateral (BA) medium over a 2 h incubation period with HT and TYR demonstrated the enterocyte-mediated absorption and metabolism of the phenolic compounds investigated. Figure 6 (panel A) shows a typical HPLC chromatogram obtained after analysis of medium from the BA side, following a 2 h incubation with HT. It was observed that the HT concentration decreases on the AP side, and that the compound can be recovered from the BA side, thus demonstrating transfer. HPLC chromatograms also show the presence of two new peaks (RT 16.18 and

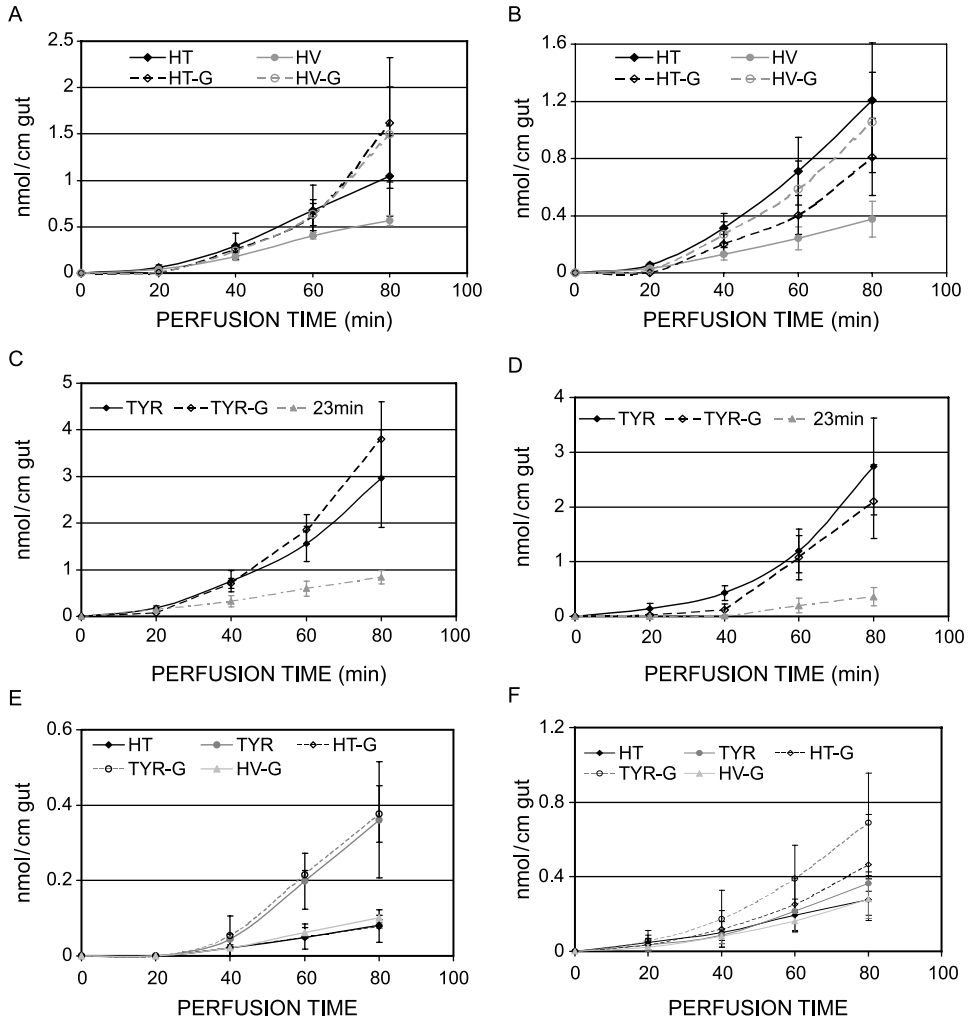

Figure 3. Cumulative absorption of olive oil polyphenols and their metabolites over 80 min through isolated rat jejunum (A, C and E) and ileum (B, D and F) after perfusion with HT (A, B), TYR (C, D) and polyphenolic fraction (E, F). Data are plotted as the mean ± SEM of three separate experiments.

21.78 min), on both, AP and BA side. The peak at 21.78 min has been identified by RT and spectra comparison with authentic standards as homovanillyl alcohol, the 3-*O*-methylated metabolite of HT. The peak at 16.18 min was identified as a glutathionyl conjugate of HT, by comparison with a synthesized standard of HT-GSH (see methods) (Figure 6B). In comparison to experiments with the isolated small intestinal model that demonstrated HT glucuronidation, using the caco-2 model the majority of the HT (90%) appeared on the basolateral side as unmetabolized HT (Figure 4D) and no glucuronidated conjugates were observed. When Caco-2 monolayers were incubated with TYR, we observed a decreasing amount of TYR in the AP, and we recovered the compound in the BA. In this case, we did not detect any new metabolite peaks in the chromatograms. In agreement with rat small intestinal studies, when Caco-2 cells where incubated with OL, we did not measure any significant decrease of compound on the AP side, and the compound was not detected on the BA side at any concentration.

Following incubation of the monolayer with the polyphenolic fraction, (a mixture containing HT and TYR), we measured a decrease in both TYR and HT on the AP side, and both compounds were detected on the BA side. No further peaks were detected on the BA side, indicating that other compounds present in the polyphenolic mixture were not transferred across the monolayer.

The rate of absorption (Figure 7) and apparent permeability coefficients (P_{app}) (Figure 5) were calculated in order to estimate the bioavailability of the compounds. TYR absorption rate was about 60% for all the concentrations loaded, and HT absorption increased with the concentration, and was between 35 and 58% (Figure 5). The P_{app} coefficients calculated ($2.18 \pm 0.37 \times 10^{-5}$ and $5.11 \pm 0.59 \times 10^{-5}$ cm/s for HT and TYR, respectively) suggest that HT and TYR are well absorbed in the small intestine following

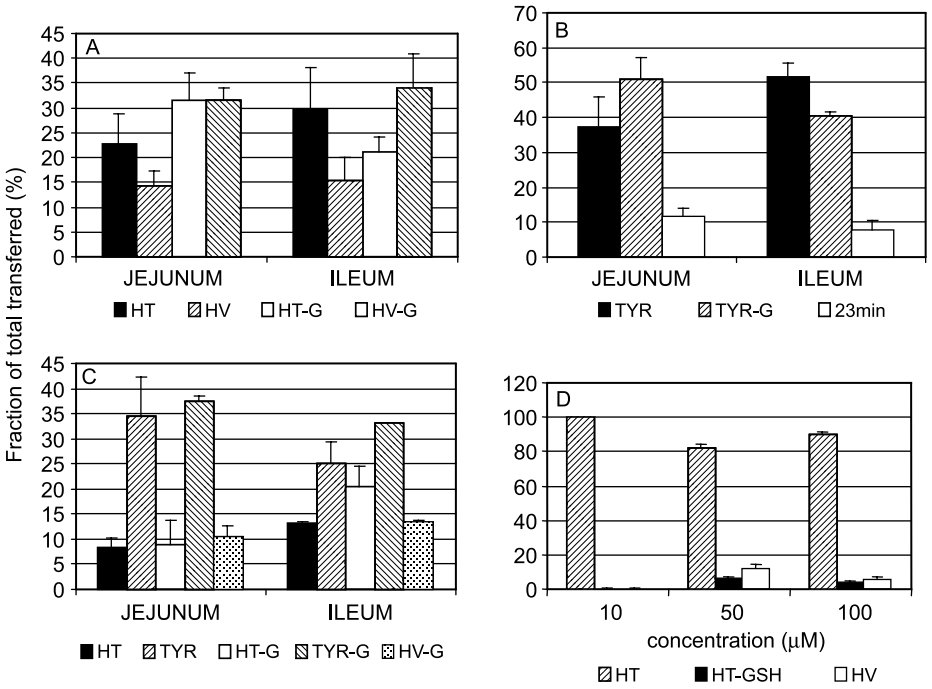

Figure 4. Relative amount of HT (A, D), TYR (B) and polyphenols (C) and their conjugates and metabolites after perfusion through the isolated rat jejunum and ileum (A, B, C) and after 2 h incubation in Caco-2 cells (D). Data are plotted as the mean ± SEM of three separate experiments.

their oral ingestion. Previous studies have positively correlated P_{app} coefficients obtained on Caco-2 cells, with the absorption in humans, indicating 100% absorption for values $>1 \times 10^{-6}$ [26]. Therefore, we propose that both HT and TYR are very well absorbed in the small intestine.

Colonic microflora fermentation: Batch culture

Previous studies have shown that OL is stable in human gastric juice and duodenal fluid [20]. Based on the fact that our data demonstrate that OL is not absorbed or metabolized in the small intestine, it is likely to reach the large intestine, where it will be subject to degradation by the colonic microflora. To gain insight into the colonic microflora-mediated biotransformations we utilized a anaerobic fermentation system. Anaerobic suspensions of human colonic micro flora were incubated with OL, the supernatants were collected at various time points and analyzed by HPLC in order to characterize and to quantify OL and OL-derived microfloral metabolites. A representative HPLC chromatogram of the ferment is shown in Figure 8 (panel A). The results demonstrate that OL was quickly and extensively degraded resulting in the formation of three compounds detected at 11.6, 36.8 and 53.9 min RT (Figure 8A). Based on the RT, the UV spectrum, and confirmed by comparisons with an authentic standard, the peak at 11.6 min was identified as HT. The two other metabolites remain to be identified. Figure 7B depicts the time-dependent biotransformation of OL by colonic microflora cultures that were established from samples obtained from three individual human donors. In agreement with previous work on the colonic micro flora-catalyzed degradation of other polyphenols [27], a comparison of the different metabolite profiles, as shown in panels B1, B2 and B3 of Figure 8, demonstrates that the biotransformation of OL was greatly influenced by individual variations in the microbial composition. However, although the time course for different donors varies (depending on the variation on microflora composition), the micro flora of all donors fully degraded OL resulting in the

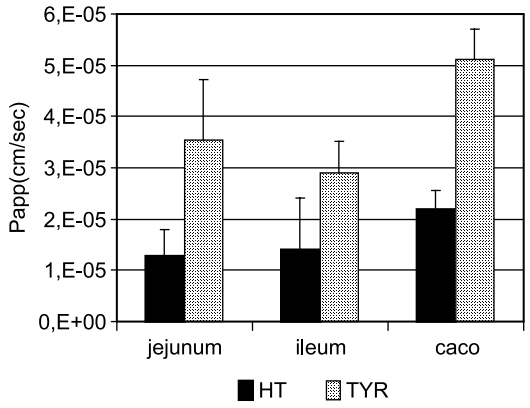

Figure 5. Apparent permeability coefficients (P_{app}) of HT and TYR in jejunum, ileum and Caco-2 monolayers. Data are plotted as the mean ± SEM ($n = 3$) and all values are significantly higher than 1×10^{-6} ($p < 0.001$).

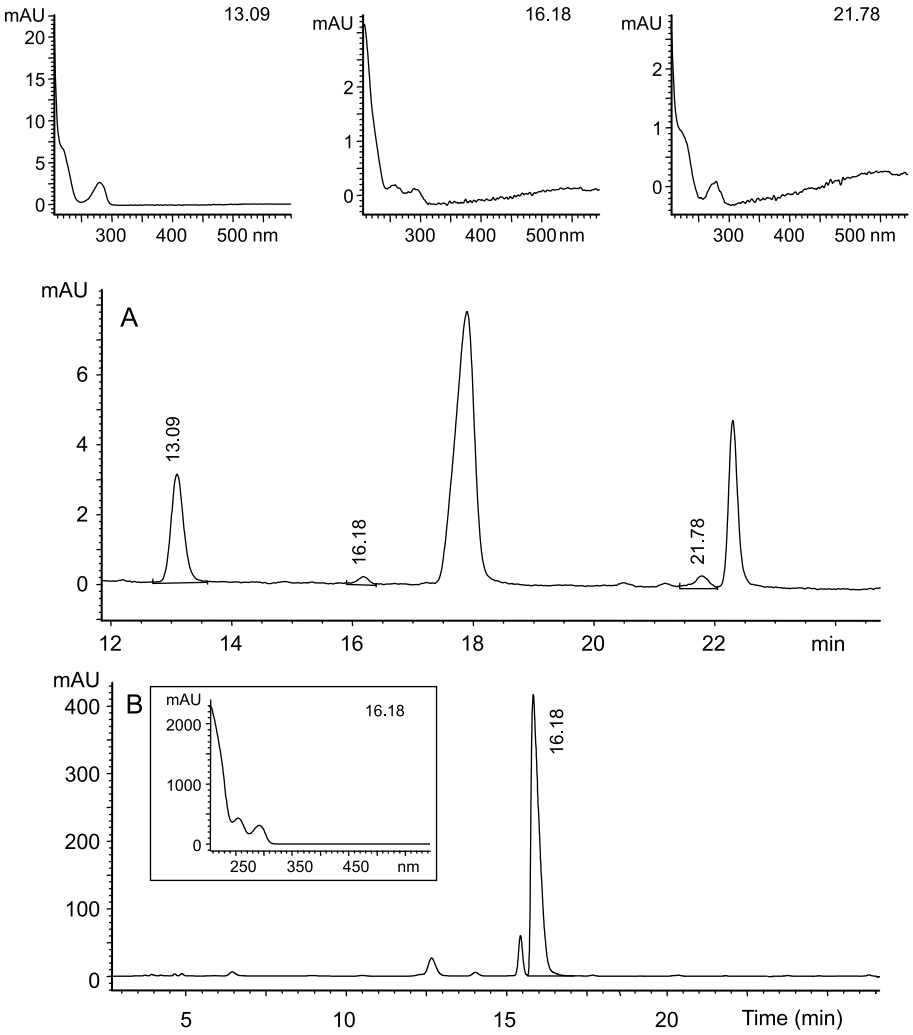

Figure 6. HPLC chromatogram with photodiode array detection (200–600 nm) of the cell culture basolateral buffer from Caco-2 monolayers after 2 h incubation with HT 100 μM (panel A). Detection was performed at 280 nm. Peaks at 13.09, 16.18 and 21.78 min RT are HT, his glutathionyl-conjugate and homovanillyl alcohol, respectively. HPLC chromatogram with photodiode array detection (200–600 nm) of the HT–GSH conjugate (panel B) obtained after HT incubation in presence of GSH and tyrosinase.

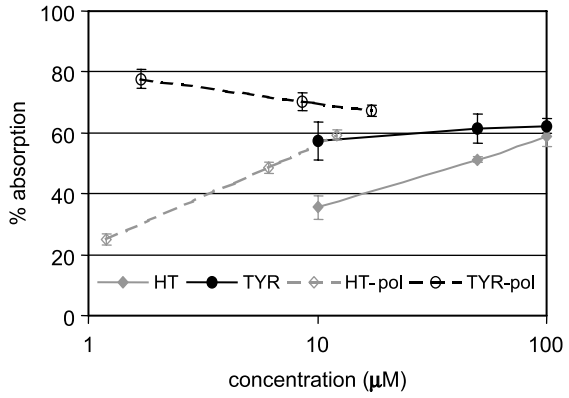

Figure 7. Absorption of HT and TYR in Caco-2 cells after 2 h incubation with the standard compounds (HT and TYR) and with the polyphenolic fraction (HT-pol and TYR-pol). Data are plotted as the mean ± SEM of three separate experiments.

appearance of three new metabolites, one of which being HT. Thus, as previously demonstrated for various phenolic acids [28,29], the micro flora-dependent hydrolysis of OL may consequently increase the bioavailability OL-derived HT via the uptake of HT through the large intestine.

Discussion

Despite the substantial body of evidence linking the *in vitro* properties of olive oil polyphenols to the health benefits associated with olive oil consumption, there are limited data on their absorption and metabolism. In order to obtain more detailed information about their mechanism of action *in vivo*, it is essential to know in which form olive oil polyphenols are in when they reach the circulation and ultimately the tissues. Presently, the vast majority of information in the

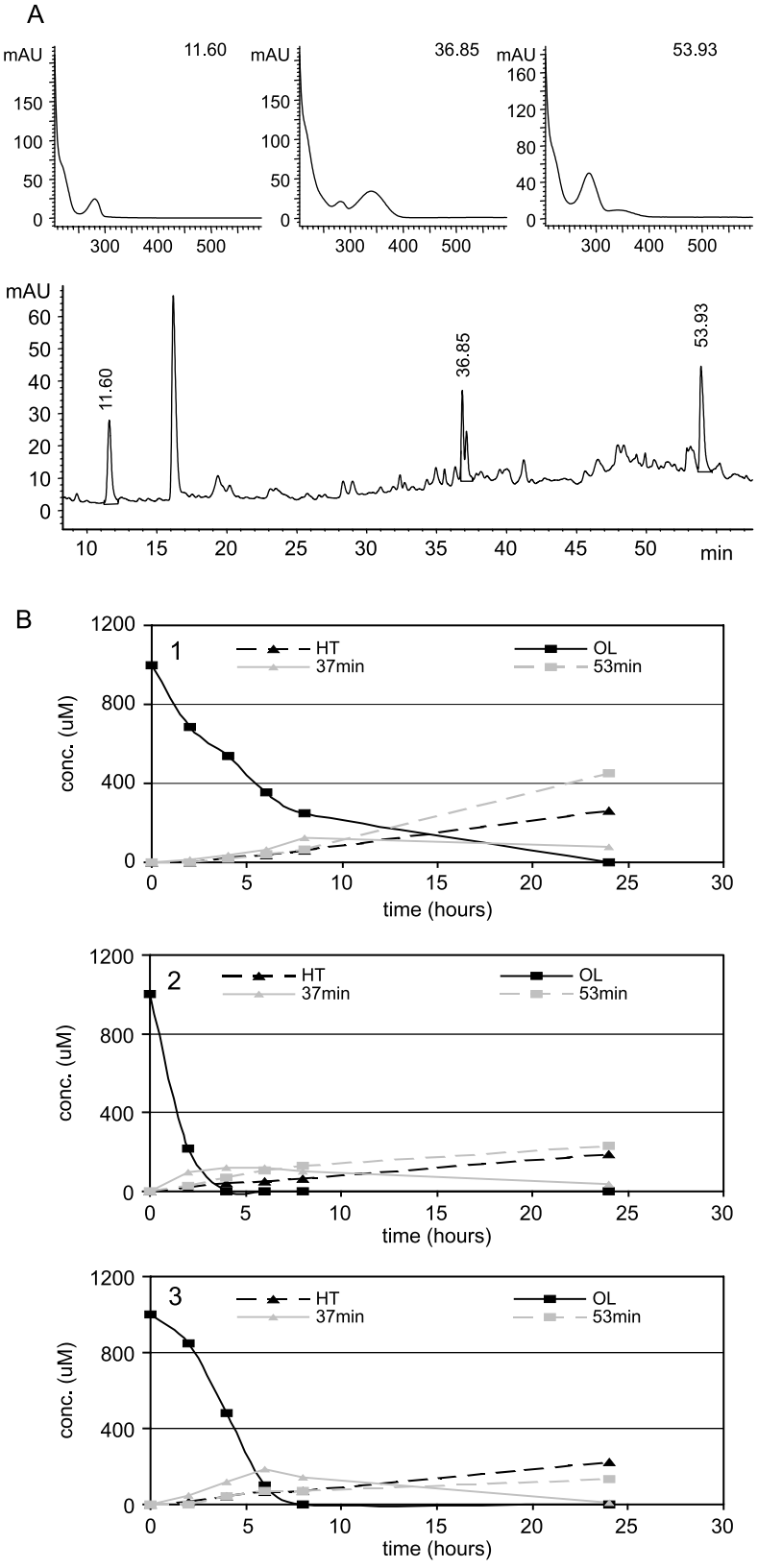

Figure 8. Example HPLC chromatograms with photodiode array detection (200–600 nm) representing the colonic biotransformation of OL after 8 h fermentation (panel A). Detection was performed at 280 nm. Time-fermentation profiles of OL and its metabolites (panel B) in three individual donors (1, 2, 3).

literature is based on analysis of blood and urine samples from animal and human studies [12–14,16,17,30–33]. However, these studies do not differentiate between the contribution of gastrointestinal metabolism and overall absorption and biotransformation of olive oil polyphenols. We observed significant non-enzymatic hydrolysis of the conjugated forms olive oil polyphenols under conditions similar to those expected during transit through the stomach *in vivo*. Although, conditions *in vivo* are more complex than in the model used here, with the food matrix affecting the precise pH, it is highly likely that the gastric environment achieves a pH of at least 2–3 for a period around 30-minutes, i.e. in order that sufficient enzymatic protein degradation may occur (pepsin). Therefore, we suggest that under such conditions the stability of complex olive oil polyphenols may be affected and could result in a significant increase in the amount of HT and TYR that arrives in the small intestine (4.75 and 3.25 times, respectively after 30 min) via the pyloroduodenal junction. In this case, higher amounts of HT and TYR may be presented for absorption in the jejunum and ileum than would be expected.

Our absorption studies agree with previous investigations which have shown the presence of HT and TYR glucuronides in urine following ingestion of olive oil polyphenols [12,13,17,31,33]. We detected HT, TYR, homovanillyl alcohol and their glucuronides in the rat small intestine model, which agreed with experiments performed in Caco-2 cells, except that no glucuronides were detected in the cellular model. This is presumably because Caco-2 cells do not possess UDP-glucuronosyl transferase activity due to their colonic origin [34]. We stress that caution should be used when interpreting absorption and metabolism data from this cell model as it could underestimate the true level of absorption of a polyphenol, especially that of the glucuronide conjugates. Similarly, use of the isolated rat small intestine model may not generate other potential human metabolites. For example, the results obtained with Caco-2 cells for HT show that the compound is also glutathione conjugated, which is not the case in the rat small intestinal segment model. As mentioned, these differences reflect different characteristics and enzymatic profiles which exist between Caco-2 cells and small intestine segments, and need to be considered when interpreting all polyphenol absorption data. Indeed, the Caco-2 model has been considered a suitable model for intestinal CYP3A4 mediated first pass metabolism, but not necessarily for UGT mediated glucuronidation [35,36]. It should also be noted that not all intestinal drug metabolizing enzymes are present in this cell line, even though Caco-2 cells have been extensively used in studies of uptake and metabolism of flavonoids [21,37,38].

Data from the two models give us a more complete understanding of how these compounds are absorbed and metabolized in humans. We have identified for the first time a glutathione conjugate of HT generated in Caco-2 cells. This metabolite may be formed either enzymatically via the action of glutathione S-transferase or non-enzymatically via oxidative metabolism of HT followed by its reaction with GSH [39]. Conjugations with thiols, such as glutathione, represent a major target for quinones, and the detoxification of quinones by GSH is generally considered to be cytoprotective. In addition, thiol conjugates of phenolics may be major bioactive forms *in vivo* and may contribute to positive health effects. We show that the majority of HT and TYR is absorbed, and underwent *O*-methylation (HT), glucuronidation (HT and TYR) and glutathionyl conjugation (HT) in the small intestine. The conversion of plant derived phenolic acids to *O*-methylated and glucuronidated metabolites in the small intestine [23] agrees with previous studies [12,16,19] which highlight the presence of these metabolites in plasma and urine after oral administration. Furthermore, in our experiments we did not reveal the presence of homovanillic acid, 3-hydroxy-4-methoxy phenylacetic acid, 2-(3,4-dimethoxyphenyl)-ethanol and sulfate-conjugate metabolites, HT metabolites found in rat urine [19], suggesting that these metabolites are formed after transport across the small intestine, most probably in the liver.

OL was not absorbed in the parental form in the small intestine and was not degraded under acidic conditions. Consequently it is likely to reach the large intestine, where it may be subjected to rapid degradation by the colonic microflora. Three major degradation products were produced by the microflora, one of them identified as being HT. Metabolism by colonic bacterial species may have the effect of increasing overall HT bioavailability, as released HT can be absorbed in the colon, as has been shown for other phenolic acids [28,29]. In addition, OL itself may possess potential prebiotic properties if bacterial groups, such as *Bifidobacteria* and *Lactobacillus*, may utilize it as a carbon source, but others such as *Clostridium* and *E. coli* cannot. Due to the rapid rate of OL fermentation in the gut model, future investigations are planned to investigate whether OL fermentation by colonic microflora can result in potential "prebiotic" changes in microbial composition.

Although metabolic processes in the small intestine may act to decrease the bioavailability and consequently the biological effects of native polyphenols, such as HT and TYR, their resultant metabolites may be capable of exerting biological effects *in vivo*. For example, Tuck et al. [19] reported that the radical scavenging potency of homovanillyl alcohol was similar to HT and that of the 3-*O*-glucuronide

conjugate was more potent when screened in an *in vitro* assay system. Whilst there has been a major focus on the antioxidant properties, there is emerging evidence that plant derived polyphenols, in particular flavonoids, and their *in vivo* metabolites can also modulate the activity of specific proteins involved in intracellular signaling pathways [40]. Many investigations indicate that flavonoids may interact within the mitogen-activated protein kinase (MAP kinase) signaling pathway [41,42] and it is possible that through oxidative mechanisms phenolic acids may act in the same way. As HT, TYR and their metabolites are relatively well absorbed in the small intestine compared to flavonoids, future investigations will center on their potential cellular actions, as has been shown for other plant derived polyphenol metabolites [39,41,43–45].

Our study provides additional information regarding the breakdown of complex olive oil polyphenols in the GI tract, in particular the stomach and the large intestine. We provide novel evidence for the breakdown of complex secoirids derivatives of olive oil polyphenols in a physiological time frame in the stomach. This gastric biotransformation effectively increases the relative amount of HT and TYR entering the small intestine. We also identify a new metabolite of HT (glutathione conjugated) and highlight the importance of comparing the transfer and metabolism of polyphenols in two different models of the small intestine. Finally, we show for the first time that although OL (a major olive oil polyphenol) is not absorbed in the small intestine it is rapidly degraded by the colonic microflora to yield HT, which may then be absorbed.

Acknowledgements

This work was supported by PIC-Interreg III, the Medical Research Council (G0400278/NI02) and the BBSRC (grants: BB/C518222/1 and 45/D15524). We also thank Dr J. Vulevic and Professor G. Gibson for their help with the colonic metabolism studies.

References

[1] Braga C, La Vecchia C, Franceschi S, Negri E, Parpinel M, Decarli A, Giacosa A, Trichopoulos D. Olive oil, other seasoning fats, and the risk of colorectal carcinoma. Cancer 1998;82:448–453.

[2] Keys A. Mediterranean diet and public health: Personal reflections. Am J Clin Nutr 1995;61:1321S–1323S.

[3] Keys A, Menotti A, Karvonen MJ, Aravanis C, Blackburn H, Buzina R, Djordjevic BS, Dontas AS, Fidanza F, Keys MH, et al. The diet and 15-year death rate in the seven countries study. Am J Epidemiol 1986;124:903–915.

[4] Owen RW, Haubner R, Wurtele G, Hull E, Spiegelhalder B, Bartsch H. Olives and olive oil in cancer prevention. Eur J Cancer Prev 2004;13:319–326.

[5] de la Puerta R, Ruiz Gutierrez V, Hoult JR. Inhibition of leukocyte 5-lipoxygenase by phenolics from virgin olive oil. Biochem Pharmacol 1999;57:445–449.

[6] Deiana M, Aruoma OI, Bianchi ML, Spencer JPE, Kaur H, Halliwell B, Aeschbach R, Banni S, Dessi MA, Corongiu FP. Inhibition of peroxynitrite dependent DNA base modification and tyrosine nitration by the extra virgin olive oil-derived antioxidant hydroxytyrosol. Free Radic Biol Med 1999; 26:762–769.

[7] Manna C, Galletti P, Cucciolla V, Montedoro G, Zappia V. Olive oil hydroxytyrosol protects human erythrocytes against oxidative damages. J Nutr Biochem 1999;10:159–165.

[8] Marrugat J, Covas MI, Fito M, Schroder H, Miro-Casas E, Gimeno E, Lopez-Sabater MC, de la Torre R, Farre M. Effects of differing phenolic content in dietary olive oils on lipids and LDL oxidation—a randomized controlled trial. Eur J Nutr 2004;43:140–147.

[9] Salami M, Galli C, De Angelis L, Visioli F. Formation of F2-isoprostanes in oxidized low density lipoprotein: Inhibitory effect of hydroxytyrosol. Pharmacol Res 1995;31:275–279.

[10] Visioli F, Caruso D, Galli C, Viappiani S, Galli G, Sala A. Olive oils rich in natural catecholic phenols decrease isoprostane excretion in humans. Biochem Biophys Res Commun 2000;278:797–799.

[11] Visioli F, Galli C. Oleuropein protects low density lipoprotein from oxidation. Life Sci 1994;55:1965–1971.

[12] Miro-Casas E, Covas MI, Farre M, Fito M, Ortuno J, Weinbrenner T, Roset P, de la Torre R. Hydroxytyrosol disposition in humans. Clin Chem 2003;49:945–952.

[13] Miro-Casas E, Covas MI, Fito M, Farre-Albadalejo M, Marrugat J, de la Torre R. Tyrosol and hydroxytyrosol are absorbed from moderate and sustained doses of virgin olive oil in humans. Eur J Clin Nutr 2003;57:186–190.

[14] Miro-Casas E, Farre Albaladejo M, Covas MI, Rodriguez JO, Menoyo Colomer E, Lamuela Raventos RM, de la Torre R. Capillary gas chromatography-mass spectrometry quantitative determination of hydroxytyrosol and tyrosol in human urine after olive oil intake. Anal Biochem 2001;294:63–72.

[15] Visioli F, Galli C, Bornet F, Mattei A, Patelli R, Galli G, Caruso D. Olive oil phenolics are dose-dependently absorbed in humans. FEBS Lett 2000;468:159–160.

[16] Visioli F, Galli C, Grande S, Colonnelli K, Patelli C, Galli G, Caruso D. Hydroxytyrosol excretion differs between rats and humans and depends on the vehicle of administration. J Nutr 2003;133:2612–2615.

[17] Caruso D, Visioli F, Patelli R, Galli C, Galli G. Urinary excretion of olive oil phenols and their metabolites in humans. Metabolism 2001;50:1426–1428.

[18] D'Angelo S, Manna C, Migliardi V, Mazzoni O, Morrica P, Capasso G, Pontoni G, Galletti P, Zappia V. Pharmacokinetics and metabolism of hydroxytyrosol, a natural antioxidant from olive oil. Drug Metab Dispos 2001;29:1492–1498.

[19] Tuck KL, Hayball PJ, Stupans I. Structural characterization of the metabolites of hydroxytyrosol, the principal phenolic component in olive oil, in rats. J Agric Food Chem 2002;50:2404–2409.

[20] Vissers MN, Zock PL, Roodenburg AJ, Leenen R, Katan MB. Olive oil phenols are absorbed in humans. J Nutr 2002;132:409–417.

[21] Manna C, Galletti P, Maisto G, Cucciolla V, D'Angelo S, Zappia V. Transport mechanism and metabolism of olive oil hydroxytyrosol in Caco-2 cells. FEBS Lett 2000;470: 341–344.

[22] Fisher RB, Gardner ML. A kinetic approach to the study of absorption of solutes by isolated perfused small intestine. J Physiol 1974;241:211–234.

[23] Spencer JPE, Chowrimootoo G, Choudhury R, Debnam ES, Srai SK, Rice-Evans C. The small intestine can both absorb

and glucuronidate luminal flavonoids. FEBS Lett 1999;458: 224–230.

[24] Spencer JPE, Jenner P, Daniel SE, Lees AJ, Marsden DC, Halliwell B. Conjugates of catecholamines with cysteine and GSH in Parkinson's disease: Possible mechanisms of formation involving reactive oxygen species. J Neurochem 1998;71:2112–2122.

[25] Kim M. Absorption of polyethylene glycol oligomers (330-1 122 Da) is greater in the jejunum than in the ileum of rats. J Nutr 1996;126:2172–2178.

[26] Artursson P, Karlsson J. Correlation between oral drug absorption in humans and apparent drug permeability coefficients in human intestinal epithelial (Caco-2) cells. Biochem Biophys Res Commun 1991;175:880–885.

[27] Rechner AR, Smith MA, Kuhnle G, Gibson GR, Debnam ES, Srai SK, Moore KP, Rice-Evans CA. Colonic metabolism of dietary polyphenols: Influence of structure on microbial fermentation products. Free Radic Biol Med 2004;36: 212–225.

[28] Rios LY, Gonthier MP, Remesy C, Mila I, Lapierre C, Lazarus SA, Williamson G, Scalbert A. Chocolate intake increases urinary excretion of polyphenol-derived phenolic acids in healthy human subjects. Am J Clin Nutr 2003;77:912–918.

[29] Rechner AR, Kuhnle G, Hu H, Roedig-Penman A, van den Braak MH, Moore KP, Rice-Evans CA. The metabolism of dietary polyphenols and the relevance to circulating levels of conjugated metabolites. Free Radic Res 2002;36:1229–1241.

[30] Covas MI, Miro-Casas E, Fito M, Farre-Albadalejo M, Gimeno E, Marrugat J, De La Torre R. Bioavailability of tyrosol, an antioxidant phenolic compound present in wine and olive oil, in humans. Drugs Exp Clin Res 2003;29:203–206.

[31] Miro Casas E, Farre Albadalejo M, Covas Planells MI, Fito Colomer M, Lamuela Raventos RM, de la Torre Fornell R. Tyrosol bioavailability in humans after ingestion of virgin olive oil. Clin Chem 2001;47:341–343.

[32] Tuck KL, Freeman MP, Hayball PJ, Stretch GL, Stupans I. The *in vivo* fate of hydroxytyrosol and tyrosol, antioxidant phenolic constituents of olive oil, after intravenous and oral dosing of labeled compounds to rats. J Nutr 2001;131: 1993–1996.

[33] Visioli F, Caruso D, Plasmati E, Patelli R, Mulinacci N, Romani A, Galli G, Galli C. Hydroxytyrosol, as a component of olive mill waste water, is dose- dependently absorbed and increases the antioxidant capacity of rat plasma. Free Radic Res 2001;34:301–305.

[34] Le Ferrec E, Chesne C, Artusson P, Brayden D, Fabre G, Gires P, Guillou F, Rousset M, Rubas W, Scarino ML. *In vitro* models of the intestinal barrier. The report and recommendations of ECVAM workshop 46. European centre for the validation of alternative methods. Altern Lab Anim 2001;29:649–668.

[35] Fisher MB, Paine MF, Strelevitz TJ, Wrighton SA. The role of hepatic and extrahepatic UDP-glucuronosyltransferases in human drug metabolism. Drug Metab Rev 2001;33:273–297.

[36] Gregory PA, Lewinsky RH, Gardner-Stephen DA, Mackenzie PI. Regulation of UDP glucuronosyltransferases in the gastrointestinal tract. Toxicol Appl Pharmacol 2004;199: 354–363.

[37] Walgren RA, Lin JT, Kinne RK, Walle T. Cellular uptake of dietary flavonoid quercetin 4′-beta-glucoside by sodium-dependent glucose transporter SGLT1. J Pharmacol Exp Ther 2000;294:837–843.

[38] Walgren RA, Walle UK, Walle T. Transport of quercetin and its glucosides across human intestinal epithelial Caco-2 cells. Biochem Pharmacol 1998;55:1721–1727.

[39] Spencer JPE, Kuhnle GG, Williams RJ, Rice-Evans C. Intracellular metabolism and bioactivity of quercetin and its *in vivo* metabolites. Biochem J 2003;372:173–181.

[40] Williams RJ, Spencer JPE, Rice-Evans C. Flavonoids: Antioxidants or signalling molecules? Free Radic Biol Med 2004;36:838–849.

[41] Spencer JPE, Rice-Evans C, Williams RJ. Modulation of pro-survival Akt/protein kinase B and ERK1/2 signaling cascades by quercetin and its in vivo metabolites underlie their action on neuronal viability. J Biol Chem 2003;278:34783–34793.

[42] Spencer JP, Murphy KP. Activation of cyclic AMP-dependent protein kinase is required for long-term enhancement at corticostriatal synapses in rats. Neurosci Lett 2002;329: 217–221.

[43] Spencer JPE, Abd-el-Mohsen MM, Rice-Evans C. Cellular uptake and metabolism of flavonoids and their metabolites: Implications for their bioactivity. Arch Biochem Biophys 2004;423:148–161.

[44] Spencer JPE, Schroeter H, Crossthwaithe AJ, Kuhnle G, Williams RJ, Rice-Evans C. Contrasting influences of glucuronidation and *O*-methylation of epicatechin on hydrogen peroxide-induced cell death in neurons and fibroblasts. Free Radic Biol Med 2001;31:1139–1146.

[45] Spencer JPE, Schroeter H, Kuhnle G, Srai SK, Tyrrell RM, Hahn U, Rice-Evans C. Epicatechin and its *in vivo* metabolite, 3′-*O*-methyl epicatechin, protect human fibroblasts from oxidative-stress-induced cell death involving caspase-3 activation. Biochem J 2001;354:493–500.